Surface Catalysis

Polymerization on Stepped Surfaces: Alignment of Polymers and Identification of Catalytic Sites**

*Alex Saywell, Jutta Schwarz, Stefan Hecht, and Leonhard Grill**

Stepped surfaces have widely been used as model catalysts as they provide active sites[1,2] which trigger many catalytic processes.[3,4] Molecular-dissociation processes on surfaces are expected to be sensitive to the surface structure and occur preferentially at defects, such as step edges and kinks. Various surface-science techniques that average over the entire surface have been employed for the investigation of catalytic properties.[3–6] Although such studies demonstrate the catalytic activity of a surface in general, they do not offer site-specific information about the exact location of the reaction. Scanning tunneling microscopy (STM) provides a local probe, allowing site-specific information to be obtained about the structure and location of active sites on a catalytically active surface with atomic resolution.[7–10] STM studies have allowed the direct observation of the active sites of heterogeneous catalysts, as shown for the dissociation of nitric oxide on a ruthenium (0001) surface,[10] where the dissociation process was found to occur along steps, but the difference in reactivity between step edges and kinks is not clear.[11] The majority of STM studies in catalysis have focused on small molecules, such as diatomic species,[10] with relatively few studies investigating the reactivity of larger organic molecules. The largest molecule investigated to date is thiophene on MoS_2 nanoclusters.[12]

The deposition of complex molecules, potentially carrying an intrinsic function, onto stepped surfaces has attracted much attention, especially with regard to templated supra-molecular structures.[13] Laterally ordered structures have been studied on various stepped gold surfaces with (111) terraces,[14–16] but oligomers or polymers have not been investigated to date. Herein we study the adsorption of α,ω-dibromoterfluorene (DBTF) molecules on a stepped gold surface. Low-temperature STM under ultrahigh vacuum (UHV) conditions is used to locally determine both the molecular adsorption geometry and the site-specific catalytic

activity of the step edges. We identify the step-edge kinks as the active sites in the catalytic process, because these defects promote the selective C−Br bond dissociation at specific locations within the DBTF molecule. Thermally induced polymerization leads to the formation of chains, which align along the step edges in a predefined orientation. This system thus provides catalytically active sites as well as an anisotropic structure for the alignment of both the monomer precursors and the polymer products.

For our studies, a gold surface with (10,7,7) orientation was used (experimental details in Supporting Information). This vicinal Au(111) surface has a misorientation angle of approximately 9° and {100}-orientated microfacets.[17] It provides straight step edges along the [0$\bar{1}$1] direction, separate flat terraces with (111) orientation, terrace widths (W_t) of around 1.4 nm[18] (Figure 1a), and is thus suitable for the adsorption of one row of molecules along each terrace. STM images of the clean surface show these terraces with an average width of 1.48 ± 0.07 nm (Figure 1b). In agreement
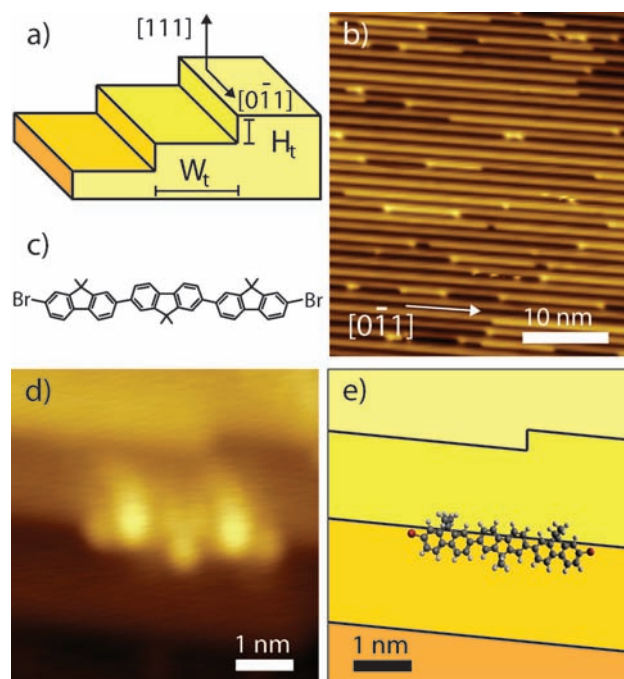

Figure 1. a) Scheme showing the structure and crystallographic directions of the Au(10,7,7) surface ($W_t \approx 1.4$ nm, $H_t = 0.235$ nm). b) STM image of the small 1.48 ± 0.07 nm width terraces of the Au(10,7,7) surface ($V_{\text{tip-bias}} = +400$ mV, $I_{\text{tunnel}} = 0.52$ nA). Arrow = [0$\bar{1}$1] direction c) Structural formula of DBTF. d) STM image showing DBTF adsorbed at a step edge ($V_{\text{tip-bias}} = +400$ mV, $I_{\text{tunnel}} = 0.55$ nA). e) Scheme showing the proposed adsorption geometry of DBTF on a straight region of a step edge.

[*] Dr. A. Saywell, Dr. L. Grill
Department of Physical Chemistry
Fritz Haber Institute of the Max Planck Society
Faradayweg 4–6, 14195 Berlin (Germany)
E-mail: lgr@fhi-berlin.mpg.de
Homepage: http://www.fhi-berlin.mpg.de/pc/grill/

J. Schwarz, Prof. S. Hecht
Department of Chemistry, Humboldt-Universität zu Berlin
Brook-Taylor-Strasse 2, 12489 Berlin (Germany)

with previous studies of vicinal Au surfaces,[18] we also observe the presence of wider terraces with widths of 4.0 ± 0.6 nm (see Supporting Information).

After deposition of DBTF (structural formula shown in Figure 1c) onto the Au(10,7,7) surface, each DBTF molecule may easily be identified by bright features (see STM image in Figure 1d) that correspond to the dimethyl groups[19,20] attached to each of the three fluorene units. On the two termini of the molecule two lobes can be seen in the STM image, these correspond to the Br atoms as determined by comparison with the gas-phase dimensions. Note that the presence (or absence) of these Br atoms can be determined from line profiles taken over the molecules (see Supporting Information).

The STM images reveal that there is a favored adsorption geometry for the DBTF molecules at the step edges (Figure 1e). If the angle between the major axis of the molecule and the direction of the step edge is measured for several molecules (Figures 2a,b), two characteristic adsorption geo-
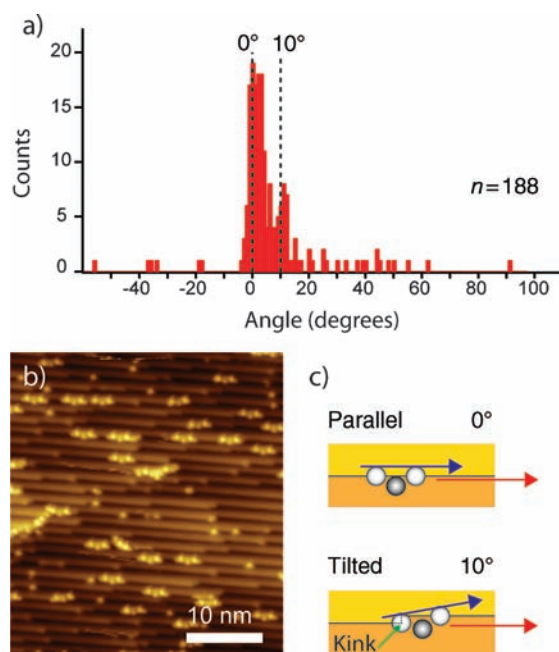
The attachment of halogen substituents to molecular building blocks is an efficient way to enable on-surface synthesis, that is, to polymerize molecules directly on a surface,[21] and various macromolecules have been formed in this manner.[19–27] Depending on the surface, the temperature, and the halogen species, the catalytic activity of the surface can lead to spontaneous molecular activation upon adsorption.[27–29] In the case of DBTF, it has been shown that the molecules remain intact after deposition onto the Au(111) surface at room temperature.[19] On the stepped Au(10,7,7) surface however, we find that almost every second molecule ($44 \pm 6\%$) has had either one (or both) of their two peripheral Br atoms removed after deposition at room temperature. This stark contrast indicates the catalytic activity of the step edges of the Au surface, which is absent on the flat (111) surface. Step-edge kink sites are of particular interest in this context, because they are proposed to be the most reactive regions along step edges owing to their low coordination as predicted by theory.[11] The only experimental study on kink defects as active sites to date is a non-local study on the reactions of *n*-heptane catalyzed by platinum single-crystal surfaces.[30]

Two kinds of kink sites, which we name I and II, may exist at a step edge, in analogy to different enantiomers of chiral objects (Figure 3a). On our Au(10,7,7) surface, there are three possible defect sites: straight steps, kink I, and kink II (Figures 3a,b). The majority of the kink sites observed in
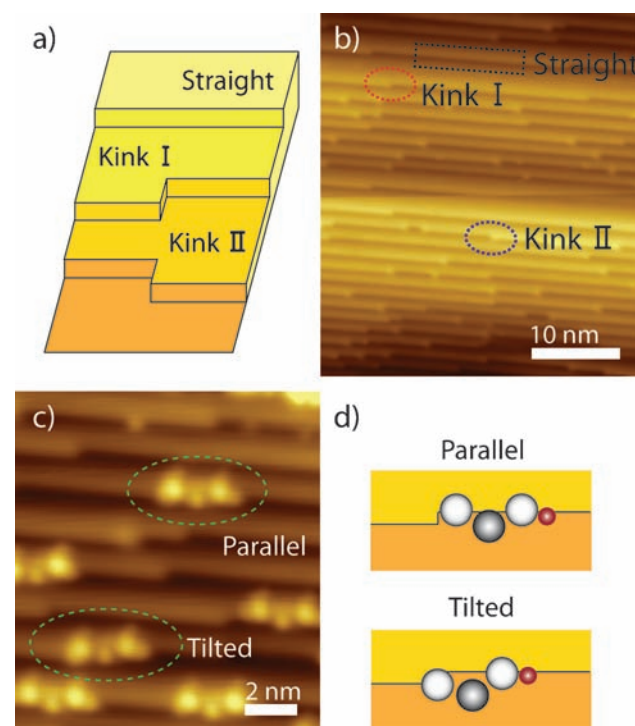
Figure 2. a) Histogram showing the angular distribution of DBTF molecules adsorbed at the Au(10,7,7) step edges and kink sites. b) Overview STM image of DBTF molecules adsorbed on the step edges ($V_{\text{tip-bias}} = +400$ mV, $I_{\text{tunnel}} = 0.55$ nA). c) Scheme showing the measured angles between the step direction and the molecular long axis for molecules adsorbed on straight regions of the step edge (parallel) and at kink sites (tilted).

Figure 3. a) Scheme showing the two types of step-edge kinks present on the surface and a straight region of the step edge. b) STM image showing examples of the kink I and kink II step-edge defects ($V_{\text{tip-bias}} = +200$ mV, $I_{\text{tunnel}} = 1.00$ nA). c) STM image showing several DBTF molecules adsorbed at kink I sites ($V_{\text{tip-bias}} = -600$ mV, $I_{\text{tunnel}} = 0.55$ nA), highlighted molecules adsorbed at kink I sites have had their 'left' Br atom dissociated. d) Scheme showing molecules in parallel and tilted orientations at a kink I step-edge defect.

metries are found. The dominant peak centered at 0°, that is, parallel to the step, is assigned to molecules that adsorb at straight regions, shown in Figure 2c. The precise adsorption geometry is determined from molecular height profiles (see Supporting Information). However, there is a second peak at approximately 10°, which reflects molecules adsorbed at kink sites of the step edge (see Figure 2c and Supporting Information).

these experiments are of type kink I (around 95 %), while only about 5 % are of kink II type, which we attribute to a slight misorientation of the surface during sample cutting, and therefore our analysis focuses on type I kink sites. At room temperature we expect kinks on the Au(10,7,7) surface to be mobile along the step edge, in analogy to vicinal Cu(111) surfaces.[31,32] Therefore adatoms, detached from kink I and kink II defects and diffusing in opposite directions along a step edge, may meet and form an island which has two new kinks (one of each type). However, neither the diffusion of kinks nor the formation of new pairs of kinks should affect the relative abundances of the two types of kink sites observed on the surface. Figure 3c shows several DBTF molecules adsorbed at the step edges of the Au(10,7,7) surface, where they may be observed in parallel or tilted orientations. The two highlighted molecules are adsorbed at the kink-I-type defects and in both cases the right Br atom is still attached to the molecule while the left Br atom has dissociated (as sketched in Figure 3d).

If the number and position of Br atoms attached to each molecule is studied for the different kinds of adsorption sites (Figure 4a), an interesting observation is made. We compare
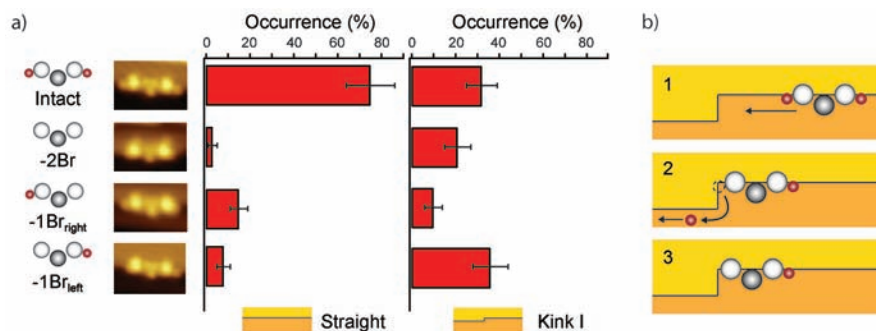

Figure 4. a) The relative occurrence of the different possibilities of Br atom removal for DBTF molecules adsorbed at straight ($n = 102$) and kink I sites ($n = 77$). b) Our proposed model for the catalytic activity of the kink sites (see text for details).

molecules at straight step edges and at the kink I sites, assuming negligible diffusion of molecules between step edges. This assumption is based on the very low occurrence of polymer structures, which would be present in much higher quantities if activated molecules (i.e. after Br atom dissociation) were able to move to other step edges and react with each other. It can be seen in Figure 4a that at the straight edges the majority of molecules ($75 \pm 11 \%$) still carry both Br atoms. The configurations with only one Br attached to the molecule are each present in rather low abundances ($-1 Br_{right}$ $15 \pm 4 \%$, $-1 Br_{left}$ $8 \pm 3 \%$). The completely activated molecule with both Br atoms dissociated is very rarely present at the straight edge ($3 \pm 2 \%$).

In contrast, Br atom dissociation occurs much more readily for molecules at the kink sites (right histogram in Figure 4a). The number of partially or completely activated molecules is greatly increased, with a corresponding decrease in intact molecules (only $32 \pm 7 \%$). An important feature is the remarkable difference between molecules that have lost

one Br atom at their left ($-1 Br_{left}$) versus their right ($-1 Br_{right}$) end; substantially more molecules have lost the Br atom at the terminus that points towards the kink defect ($36 \pm 8 \%$ compared to $10 \pm 4 \%$). The significant asymmetry between the removal of left and right Br atoms reflects the asymmetric abundance of kink types I (95 %) and II (5 %). The correlation between the high number of kink I sites and the preference for the cleaving of the left C−Br bond reveals that the kink site enhances Br dissociation, thus acting as the catalytically active site of the surface. Alternative interpretations, for example, molecular activation at a straight area of the step, which would produce equal amounts of both $-1 Br_{left}$ and $-1 Br_{right}$ DBTF, and subsequent diffusion towards and adsorption at the kink site (potentially with unequal adsorption energies depending on which molecular terminus has been activated) appear implausible, as they do not explain the strong asymmetry seen in the Br atom dissociation of the two molecular termini for all molecules on the surface. Note that rotation of the molecules at room temperature seems unlikely to occur because this would cause a homogeneous distribution of molecules with a single Br atom (i.e. about the same number of $-1 Br_{left}$ as $-1 Br_{right}$), even in the case of asymmetric activation. Because the sample is at room temperature for several hours, this would be sufficient time to equilibrate the abundance of $-1 Br_{left}$ and $-1 Br_{right}$ if they were able to freely rotate.

Therefore, we propose the mechanism shown in Figure 4b: 1) Intact molecules diffuse along the step edge, the direction of the lowest energy barrier, until they arrive at a kink site, which provides a local environment in which the Br atom at the terminus is catalytically cleaved (2). Finally, the activated molecule remains adsorbed at the kink site (3), because its diffusion barrier is increased after activation, presumably because of bonding interactions between a kink gold atom and the terminal carbon atom of the activated DBTF. It should be noted that our model does not preclude the activation of molecules on straight regions of the step edge, in addition to those activated at kink sites, and their subsequent diffusion to kink sites, as an additional yet less-efficient pathway. Our proposed mechanism is also in agreement with the low occurrence of polymers (ten molecules out of 248 were observed to be present within dimers and no longer chains were found), despite molecular activation of DBTF. To form a polymer, an activated molecule must diffuse along a step edge to collide with another molecule, which must have been activated on the opposite end to allow the activated carbon atoms to interact. As this particular surface is cut asymmetrically (leading to more kink I sites than kink II), it promotes asymmetric activation (i.e. the removal of the left Br atom of the molecule), and therefore covalent linking is unlikely, because of the low probability of molecules with oppositely removed Br atoms meeting.

In addition to providing catalytic sites for the removal of Br atoms from DBTF, the step edges of the Au(10,7,7) surface may also be used to align the polymers produced by thermal activation of the DBTF monomer units. Figure 5a shows the
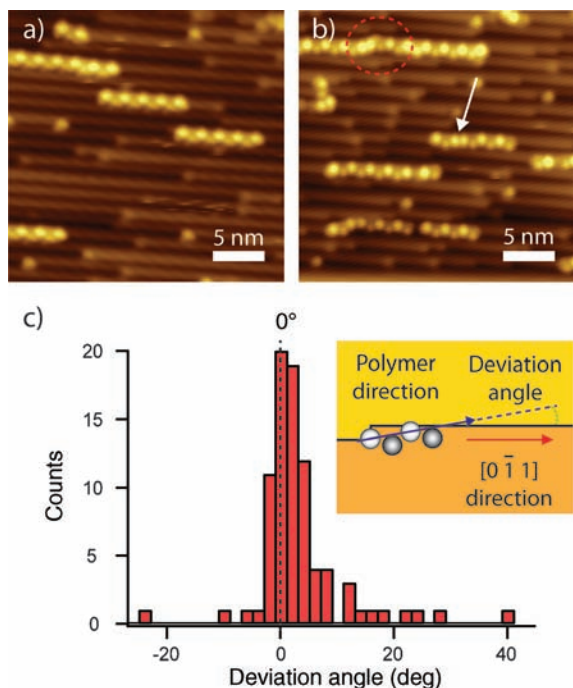

Figure 5. a) STM image of polyfluorene chains after annealing the sample at 523 K ($V_{\text{tip-bias}} = +400$ mV, $I_{\text{tunnel}} = 0.49$ nA), chains align along the step edges. b) STM image ($V_{\text{tip-bias}} = +400$ mV, $I_{\text{tunnel}} = 0.49$ nA) showing an "up""up" type defect (arrow) and a polymer chain, which is continuous over a kink (dashed ellipse). c) The angular deviation for adsorbed polymer chains ($n = 84$). Inset shows definitions for the measured quantities.

Au(10,7,7) surface after molecular deposition and subsequent annealing at 523 K (for 5 min), with fluorene chains produced by way of the on-surface synthesis process.[19,20] Statistical analysis of the STM images shows that prior to annealing the majority of the structures are isolated monomer units, with only $4 \pm 1\%$ of the molecules being present within dimers. In contrast, after annealing $87 \pm 6\%$ of the molecules are part of a polymer chain with two or more monomer units. The polymer chains show a striking affinity for adsorption along the step edges, similar to the DBTF monomers (i.e. prior to annealing). Detailed analysis of the angle between the step-edge direction and the direction of the polymer chain (Figure 5c) reveals that the majority of the polymers run continuously along a step edge. This highly regular orientation is attributed to the alignment of the individual monomer units, which is driven by the preferential adsorption geometry discussed above. The observed polymer length on the Au-(10,7,7) surface is found to be reduced compared to the Au(111) case,[19] probably because of the higher diffusion barriers on the stepped surface. We find that the polymers align along the step edges, adjacent to both the narrow and the wide terraces of the surface, and longer polymers are

found on the step edges adjacent to the wide terraces (see Supporting Information). Note that the polymer alignment is precisely the same over the entire macroscopic sample, because the step-edge orientation is determined by the structure of the single-crystal, in contrast to alignment along surface reconstructions.[19,23,27,33,34]

The bright features within the chain (corresponding to the dimethyl groups of the fluorene units) exhibit a "zigzag" pattern (or "up""down", referring to the position of adjacent dimethyl groups relative to the step edge; see Figure 1d,e) along the step edge (Figure 5a), corresponding to the all *anti* conformation of the polyfluorene chain (in contrast to the "up""up" case seen in Figure 5b).[19] This result shows (according to the assignment in Figure 1d) that the dimethyl groups alternate between being adsorbed on the upper and lower terraces. Prior to annealing, the majority of the monomers have both terminal dimethyl groups adsorbed on the upper terrace (Figure 1d,e), meaning that in order to produce the "zigzag" polymer structure every other DBTF monomer must rearrange so that the two outer dimethyl groups of these molecules are on the lower terrace. Interestingly this implies that the DBTF monomer units must undergo a conformational change, or a 180° rotation, during the annealing process, enabled by the higher temperatures. Our analysis reveals that after annealing almost all ($97 \pm 1\%$) adjacent dimethyl groups are present as part of a "zigzag" structure and other, non-alternating, arrangements are extremely rare (see Supporting Information). This finding demonstrates that the step-edge adsorption geometry of the monomer units is transferred to the covalently bound polymer chains. The polymer chains are also seen to be continuous over kink defects on the step edges, only resulting in a slight parallel offset before continuing to follow the same step edge (arrow in Figure 5b). Defects of the type where the polymer chain leaves the step edge are observed infrequently (only about 10% of the polymer chains).

In conclusion, we have demonstrated that the Au(10,7,7) stepped surface can be used as a template to produce highly aligned polymers. The surface steps are shown to act as catalytic sites for Br atom removal from the DBTF molecule and consequently the polymerization process, leading to efficient molecular activation in contrast to the flat Au(111) terraces. Specifically, we identify the kink defects as the catalytically active sites, as the asymmetric dissociation of Br atoms from the monomers correlates directly to the unequal abundance of kink sites.

Please note: Minor changes have been made to this manuscript since its publication in *Angewandte Chemie* Early View. The Editor.

[1] H. S. Taylor, *Proc. R. Soc. London Ser. A* **1925**, *108*, 105–111.

[2] G. Ertl, H. Knözinger, F. Schüth, J. Weitkamp, *Handbook of Heterogeneous Catalysis*, Wiley-VCH, **2008**.

[3] G. A. Somorjai, *Surf. Sci.* **1994**, *299–300*, 849–866.

[4] J. T. Yates, *J. Vac. Sci. Technol. A* **1995**, *13*, 1359–1367.

[5] A. Paul, M. Yang, B. Bent, *Surf. Sci.* **1993**, *297*, 327–344.

[6] V. Kanuru, G. Kyriakou, S. Beaumont, A. Papageorgiou, D. Watson, R. Lambert, *J. Am. Chem. Soc.* **2010**, *132*, 8081–8086.

[7] R. T. Vang, J. V. Lauritsen, E. Lægsgaard, F. Besenbacher, *Chem. Soc. Rev.* **2008**, *37*, 2191–2203.

[8] R. T. Vang, K. Honkala, S. Dahl, E. K. Vestergaard, J. Schnadt, E. Lægsgaard, B. S. Clausen, J. K. Norskov, F. Besenbacher, *Nat. Mater.* **2005**, *4*, 160–162.

[9] J. Wintterlin, S. Völkening, T. V. W. Janssens, T. Zambelli, G. Ertl, *Science* **1997**, *278*, 1931–1934.

[10] T. Zambelli, J. Wintterlin, J. Trost, G. Ertl, *Science* **1996**, *273*, 1688–1690.

[11] Z.-P. Liu, P. Hu, *J. Am. Chem. Soc.* **2003**, *125*, 1958–1967.

[12] J. V. Lauritsen, M. Nyberg, J. K. Nørskov, B. S. Clausen, H. Topsøe, E. Lægsgaard, F. Besenbacher, *J. Catal.* **2004**, *224*, 94–106.

[13] J. Kröger, N. Neel, H. Jensen, R. Berndt, R. Rurali, N. Lorente, *J. Phys. Condens. Matter* **2006**, *18*, S51-S66.

[14] A. Mäkinen, J. Long, N. Watkins, Z. Kafafi, *J. Phys. Chem. B* **2005**, *109*, 5790–5795.

[15] W. Xiao, P. Ruffieux, K. Ait-Mansour, O. Groning, K. Palotas, W. Hofer, P. Groning, R. Fasel, *J. Phys. Chem. B* **2006**, *110*, 21394–21398.

[16] M. Cañas-Ventura, W. Xiao, D. Wasserfallen, K. Mullen, H. Brune, J. Barth, R. Fasel, *Angew. Chem.* **2007**, *119*, 1846–1850; *Angew. Chem. Int. Ed.* **2007**, *46*, 1814–1818.

[17] S. Rousset, V. Repain, G. Baudot, Y. Garreau, J. Lecoeur, *J. Phys. Condens. Matter* **2003**, *15*, S3363-S3392.

[18] M. Corso, F. Schiller, L. Fernandez, J. Cordon, J. Ortega, *J. Phys. Condens. Matter* **2009**, *21*, 353001.

[19] L. Lafferentz, F. Ample, H. Yu, S. Hecht, C. Joachim, L. Grill, *Science* **2009**, *323*, 1193–1197.

[20] C. Bombis, F. Ample, L. Lafferentz, H. Yu, S. Hecht, C. Joachim, L. Grill, *Angew. Chem.* **2009**, *121*, 10151–10155; *Angew. Chem. Int. Ed.* **2009**, *48*, 9966–9970.

[21] L. Grill, M. Dyer, L. Lafferentz, M. Persson, M. V. Peters, S. Hecht, *Nat. Nanotechnol.* **2007**, *2*, 687–691.

[22] M. Xi, B. E. Bent, *J. Am. Chem. Soc.* **1993**, *115*, 7426–7433.

[23] J. A. Lipton-Duffin, O. Ivasenko, D. F. Perepichka, F. Rosei, *Small* **2009**, *5*, 592–597.

[24] M. Bieri, et al., *Chem. Commun.* **2009**, 6919–6921.

[25] M. O. Blunt, J. C. Russell, N. R. Champness, P. H. Beton, *Chem. Commun.* **2010**, *46*, 7157–7159.

[26] R. Gutzler, H. Walch, G. Eder, S. Kloft, W. M. Heckl, M. Lackinger, *Chem. Commun.* **2009**, 4456–4458.

[27] L. Lafferentz, V. Eberhardt, C. Dri, C. Africh, G. Comelli, F. Esch, S. Hecht, L. Grill, *Nat. Chem.* **2012**, *4*, 215–220.

[28] M. Bieri, et al., *J. Am. Chem. Soc.* **2010**, *132*, 16669–16676.

[29] J. L. Lin, B. E. Bent, *J. Phys. Chem.* **1992**, *96*, 8529–8538.

[30] W. D. Gillespie, R. K. Herz, E. E. Petersen, G. A. Somorjai, *J. Catal.* **1981**, *70*, 147–159.

[31] M. Giesen, G. Schulze Icking-Konert, *Surf. Sci.* **1998**, *412–413*, 645–656.

[32] M. Giesen-Seibert, H. Ibach, *Surf. Sci.* **1994**, *316*, 205–222.

[33] D. Zhong, J.-H. Franke, S. K. Podiyanachari, T. Blömker, H. Zhang, G. Kehr, G. Erker, H. Fuchs, L. Chi, *Science* **2011**, *334*, 213–216.

[34] J. A. Lipton-Duffin, J. A. Miwa, M. Kondratenko, F. Cicoira, B. G. Sumpter, V. Meunier, D. F. Perepichka, F. Rosei, *Proc. Natl. Acad. Sci. USA* **2010**, *107*, 11200–11204.